2024

Hubble Tension and Gravitational Self-Interaction

Corey Sargent
Old Dominion University, cjsargen@odu.edu

William Clark
Old Dominion University, wclar001@odu.edu

Alexander Deur
Old Dominion University

Balša Terzić
Old Dominion University, bterzic@odu.edu

Original Publication Citation

Sargent, C., Clark, W., Deur, A., & Terzić, B. (2024). Hubble tension and gravitational self-interaction. *Physica Scripta*, *99*(7), 1-9, Article 075043. https://doi.org/10.1088/1402-4896/ad570f

IOP Publishing   *Phys. Scr.* **99** (2024) 075043   https://doi.org/10.1088/1402-4896/ad570f

Physica Scripta

CrossMark

OPEN ACCESS

RECEIVED
29 December 2023

REVISED
31 May 2024

ACCEPTED FOR PUBLICATION
11 June 2024

PUBLISHED
25 June 2024

PAPER

Hubble tension and gravitational self-interaction

Corey Sargent[1,†], **William Clark**[1], **Alexandre Deur**[1,2] and **Balša Terzić**[1]

[1] Department of Physics, Old Dominion University, Norfolk, VA 23529, United States of America
[2] Department of Physics, University of Virginia, Charlottesville, VA 22901, United States of America
[†] Deceased

E-mail: deurpam@jlab.org

Keywords: cosmology, hubble constant, general relativity, dark energy, dark matter, cosmic microwave background

Abstract

One of the most important problems vexing the ΛCDM cosmological model is the Hubble tension. It arises from the fact that measurements of the present value of the Hubble parameter performed with low-redshift quantities, e.g. the Type IA supernova, tend to yield larger values than measurements from quantities originating at high-redshift, e.g. fits of cosmic microwave background radiation. It is becoming likely that the discrepancy, currently standing at 5σ, is not due to systematic errors in the measurements. Here we explore whether the self-interaction of gravitational fields in General Relativity, which are traditionally neglected when studying the evolution of the Universe, can contribute to explaining the tension. We find that with field self-interaction accounted for, both low- and high-redshift data are *simultaneously* well-fitted, thereby showing that gravitational self-interaction yield consistent H_0 values when inferred from SnIA and cosmic microwave background observations. Crucially, this is achieved without introducing additional parameters.

1. The Hubble tension

Modern cosmology began with the discovery of Hubble's law. Its central element, the present value of the Hubble parameter, H_0, has a troubled history of measurements and it is only in the last two decades that precise determinations became available. However, two types of precision measurements of H_0 are in conflict. The first type comprises observations of phenomena originating at high redshift z, principally the power spectrum of the cosmic microwave background (CMB) (Aghanim *et al* 2020a) and the baryon acoustic oscillations (BAO) (Alam *et al* 2021). The second type consists of determination of H_0 from low-z phenomena, notably using standard candles (Riess *et al* 2016) and time-delay cosmography (Wong *et al* 2020) methods. See (Abdalla *et al* 2022) for the low- and high-z methods providing H_0. The high-z phenomena yield H_0 values significantly lower than those from low-z. This is known as the 'Hubble tension' (Verde *et al* 2019, Di Valentino *et al* 2021, Abdalla *et al* 2022). The discrepancy presently reaches a 5σ significance: the combined high-z measurements yield 67.28 ± 0.60 km/s/Mpc while the combined low-z measurements yield $H_0 = 73.04 \pm 1.04$ km/s/Mpc (Riess *et al* 2022). Yet, individual low-z measurements can be as much as 6σ away (Abdalla *et al* 2022) from the most precise high-z datum, the Planck satellite result (Aghanim *et al* 2020a).

Although the Hubble tension may originate from unaccounted systematic effects (Freedman *et al* 2020), the consistency of the high-z results on the one hand, and that of the low-z results on the other, suggests that it could instead reveal a limitation of the current standard model of cosmology, the dark energy-cold dark matter model (ΛCDM) (Shah *et al* 2021, Di Valentino *et al* 2021). This would be just one of the several malaises of ΛCDM. A first worry is that detection of dark matter particles by direct (Kahlhoefer 2017) or indirect (Gaskins 2016) measurements is still wanting, with searches having almost exhausted the allowed parameter spaces of likely candidates. Furthermore, the most natural extensions of the standard model of particle physics which offer convincing dark matter candidates are mostly ruled out, e.g. minimal SUSY (Arcadi *et al* 2018). Other worries with ΛCDM include overestimating the number of globular clusters and dwarf galaxies (Klypin *et al* 1999) or the lack of uncontrived explanation for tight correlations between the supposedly sub-dominant baryonic matter and quantities characterizing galaxy dynamics, e.g. the Tully-Fisher relation (Tully and Fisher 1977), radial acceleration relation (RAR) (McGaugh *et al* 2016), or Renzo's rule (Sancisi 2004). These issues motivate developing alternatives to ΛCDM that could naturally resolve these problems. Here we follow this direction and investigate whether the Hubble tension can be understood with a model that incorporates the fact that in General Relativity (GR), gravitational fields interact with each others (field self-interaction, SI). That central feature of GR is the basis for the GR-SI model. This model currently accounts for a range of key observations traditionally ascribed to dark matter or dark energy. These include the flat rotation curves of galaxies, the luminosities of high-redshift supernovae, the anisotropies in the Cosmic Microwave Background (CMB), and the formation of large-scale structures. Crucially, this is achieved without the introduction of dark components (Deur 2009, 2019, Deur *et al* 2020, Deur 2021a, 2021b, 2022). From these and other successes we find that GR-SI needs to be tested in different regimes to better understand its utility in modern cosmology.

In the next section, we recall the physical basis of the GR-SI framework and its predictions. We then discuss how, from the perspective of the GR-SI model, a Hubble tension should arise if low- and high-z data are analyzed with ΛCDM, and why the tension is not present in GR-SI. After summarizing how the evolution of the Universe affects the CMB anisotropy observations in both the GR-SI and ΛCDM frameworks, we use GR-SI to fit luminosity distance data. This constrains the GR-SI parameters describing the effects of large-scale structure formation on the long distance propagation of gravity, effects that are encapsulated in a so-called *depletion function* $D_M(z)$ whose meaning we will briefly recall in section 2. The fit describes well the SnIA and CMB-inferred luminosity distances with a single H_0 value of 73.06 km/s/Mpc. Finally, we show in section 4 that the cosmological parameters which alleviate the Hubble tension within the GR-SI model also simultaneously fit well the CMB power spectrum. This supporting result serves as an internal consistency check for the GR-SI formalism.

2. Field self-interaction and its consequences

A defining feature of GR is that it is a non-linear theory: gravity fields interact with each other, in contrast to Newtonian gravity. The linear character of the latter allows for the field superposition principle, while in GR, the combination of fields differ from their sum since the fields interact. In fact, the GR Lagrangian $\mathcal{L}_{\rm GR} = \sqrt{\det(g_{\mu\nu})}\; g_{\mu\nu} R^{\mu\nu} \big/ (16\pi G)$ (here $g_{\mu\nu}$ is the metric, G is Newton's constant and $R_{\mu\nu}$ is the Ricci tensor) expressed in a polynomial form (Zee 2013):

$$\mathcal{L}_{\rm GR} = \sum_{n=0}^{\infty} (16\pi MG)^{n/2} [\phi^n \partial\phi\partial\phi], \tag{1}$$

Explicitly shows that a gravitational field self-interacts. Here, $\phi_{\mu\nu}$ is the gravitational field due to a unit mass and is defined as the deviation of $g_{\mu\nu}$ from a reference constant metric $\eta_{\mu\nu}$, $\phi_{\mu\nu} \equiv (g_{\mu\nu} - \eta_{\mu\nu}) \big/ \sqrt{M}$, where M is the mass of the system. For simplicity, we ignored the matter term of $\mathcal{L}_{\rm GR}$: to discuss the pure field case is sufficient. We discuss in a moment why ignoring the matter term is justified even for a matter-filled universe. The bracket in $[\phi^n \partial\phi\partial\phi]$ signifies a sum of Lorentz-invariant terms whose forms are $\phi^n \partial\phi\partial\phi$, e.g. $[\partial\phi\partial\phi]$ is the Fierz-Pauli Lagrangian of linearized GR (Fierz and Pauli 1939). Newtonian gravity is recovered if $\eta_{\mu\nu}$ is the Minkowski metric and if one keeps only the time-time component of the $n = 0$ term of equation (1): $[\partial\phi\partial\phi] \overset{\rm Newton}{=} \partial^\mu \phi_{00} \partial_\mu \phi^{00}$ and $\partial^0 \phi_{00} = 0$. The term $[\partial\phi\partial\phi]$ formalizes the free motion of the field, *viz*, it generates the two-point correlation function that gives the probability for the field to freely propagate from one spacetime point to another. The $n > 0$ terms are interaction terms and therefore cause the field SI. An analogous phenomenon occurs for the nuclear Strong Force, whose theory is Quantum Chromodynamics (QCD). Actually, the reason why GR and QCD are non-linear theories is the same: they possess several types of distinct 'charges'. For GR, they are the mass/energy, momentum and stress which are grouped under the stress-energy tensor, which then represent a rank-2 tensor charge. For QCD, they are the three color charges. This causes the fields of GR and QCD to be rank-2 tensors, i.e. non-commuting objects. This is not the case in non-linear theories like QED and Newtonian gravity which only involve scalar charges. SI terms are present in the classical Lagrangians of GR and QCD, i.e. before any quantization procedure for the later, and thus field SI is a classical phenomenon. The non-zero commutators in turn give rise to SI terms It results in GR and QCD having the same classical Lagrangian structure. Field SI is a central and conspicuous feature of QCD due to its large coupling α_s (Deur *et al* 2016). In contrast, field SI in GR is controlled by $\sim\sqrt{16\pi GM/L}$ (with L a characteristic length of the system), whose value is typically small. This makes the linear approximations of GR, e.g. the Newtonian or the Fierz-Pauli theories, adequate for most applications. However, if $\sqrt{16\pi GM/L}$ is large enough, SI *must* be accounted for: it is an unavoidable consequence of GR. In (Deur 2017) it was shown that for a typical galaxy, $\sqrt{16\pi GM/L} \simeq 10^{-2}$, which is large enough to enable SI. This is also the case for galactic clusters but need not be true for other combinations of M and L. For example, the masses and length scales of wide binary stars are not expected to exhibit any deviations from Newton in GR-SI. This expectation distinguishes GR-SI from modified Newtonian dynamics (MOND), which posits that the low acceleration regimes of wide binaries should result in noticeable deviations from Newton. In particular, MOND expects that binary stars with large separations (on the order of 10 kAU) should exhibit circular velocities around 20 percent higher than those predicted by classical Newtonian dynamics (Banik and Zhao 2018). A verification of this prediction was reported at a significance of 10σ in a study analyzing over 26,000 wide binaries from the GAIA 3DR survey (Chae 2023), although another study using the same GAIA data (Banik *et al* 2023) found the dynamics to be consistent with Newtonian gravity and attributed the initial MOND confirmation of (Chae 2023) to the way velocity uncertainties were estimated. In the realm of wide binaries, GR-SI aligns with the Newtonian (and ΛCDM) perspective, expecting no detectable self-interaction due to the relatively small masses involved. One consequence of SI in QCD is to enhance the binding of quarks, resulting in their confinement. Likewise in GR, if a galactic mass is large enough to enable SI, it would enhance the binding of galactic components in a manner that directly leads to flat galactic rotation curves (Deur 2009) without requiring dark matter. The increased binding also dispenses with the need for dark matter to account for the growth of large-scale structures (Deur 2021b). On the other hand, using Newtonian gravity to analyze systems in which SI is important overlooks the binding enhancement and produces an apparent mass discrepancy interpreted as dark matter. Importantly, SI effects cancel out in isotropic and homogeneous systems. For example, a nearly spherical galaxy has much less evidence of dark matter than a flatter, disk like galaxy (Deur 2014, Winters *et al* 2023).

Another direct and crucial consequence of the binding enhancement comes from energy conservation: the increase of binding energy inside a system must be balanced by a reduction of the gravitational energy outside of the system. In QCD, the larger binding confines quarks into hadrons, while outside hadrons, the Strong Force declines into the much weaker residual Yukawa interaction. Likewise, if SI binds more tightly massive systems, gravitation must be reduced outside these systems. Overlooking that large-distance reduction of gravity would require a compensating global repulsion in much the same way as overlooking the binding enhancement requires a compensating dark mass. The purported repulsion would then be interpreted as dark energy. To restate differently, field line collapse increases the binding energy in systems (Gross *et al* 2023), including very massive systems according to GR-SI. By energy conservation, this increase of energy inside such a system suppresses the effect of the force outside the system (Wilczek 2002, Deur 2019). This can also be easily understood as due to the fact that the force field lines are collapsed into the system and do not flow out of it anymore. This effect, originating from the pure-field sector of the theory, has an important impact on the matter part of the theory: as previously mentioned, the force is suppressed ('depleted', in GR-SI terms) between massive (matter-made) systems compared to the Newtonian expectation or to the GR expectation under the usual isotropy and homogeneity assumptions. It thus has crucial implication to the dynamics of matter, even though the phenomenon itself is a pure-field effect in origin. This depletion can explain the acceleration of the Universe without recourse to dark energy (Deur 2019) and is therefore the primary ingredient in our explanation of the Hubble tension despite originating from the pure-field sector of the theory. Likewise, In QCD, color confinement can be accurately reproduced in the pure field sector, and it is common to neglect fermionic degrees of freedom in demanding lattice gauge computations.

The GR-SI approach is not the only attempt to explain away dark energy from departure from the cosmological principle at short scales (Schander and Thiemann 2021). However, the effects of structures on the evolution of the Universe were initially investigated using Newtonian gravity within a Friedmann-Lemaître-Robertson-Walker background. Only recently did advances in numerical GR open the possibility of full GR simulations. These simulations have not yet found clear signs of important effects (Macpherson *et al* 2018, 2019, Schander and Thiemann 2021). However, they are not yet complete, as they lack e.g. the effect of the pressure of the relativistic constituent making-up the early universe, or of electromagnetic radiations. Both are necessary to the formations of the structures considered by GR-SI. Furthermore, the simulation resolution is above the Mpc scale, much larger that the characteristic scale over which the field SI enfolds in GR-SI (sub-kpc for galaxies (Deur 2021a) and tens of kpc for galaxy clusters (Deur 2009)). Therefore, these simulations are not yet sensitive to the mechanism central to GR-SI. Such approaches can be qualified as top-down, aiming to directly compute the effects of the forming structures on the evolution of the Universe. GR-SI is a bottom-up approach, first computing non-perturbatively GR's SI, with numerical simulations or models, at the small scales characterizing galaxies, and then propagating phenomenologically their consequence for the evolution of the Universe. Another challenge to overcome is the non-perturbative nature of the SI effect, which has already been notoriously difficult to compute in the case of QCD and is still not fully understood.

The enhanced binding of structures in GR-SI, *viz*, the *local* effect of SI, is computed starting from GR's Lagrangian, equation (1) (Deur 2009, 2017). The large-distance suppression of gravity, *viz*, the *global* effect, is evaluated effectively using a *depletion function* $D_M(z)$ that originates from lifting the traditional assumptions that the Universe is isotropic and homogeneous (Deur 2019). If $D_M = 0$, gravity is fully quenched at large-distance while for D_M=1 there is no net SI effect. Thus, $D_M(z) \approx 1$ for the early universe since it was nearly isotropic and homogeneous. In contrast, the large-scale structures of the present universe entail $D_M(z \approx 0) < 1$. The form of $D_M(z)$ first proposed in (Deur 2019) can be approximated by:

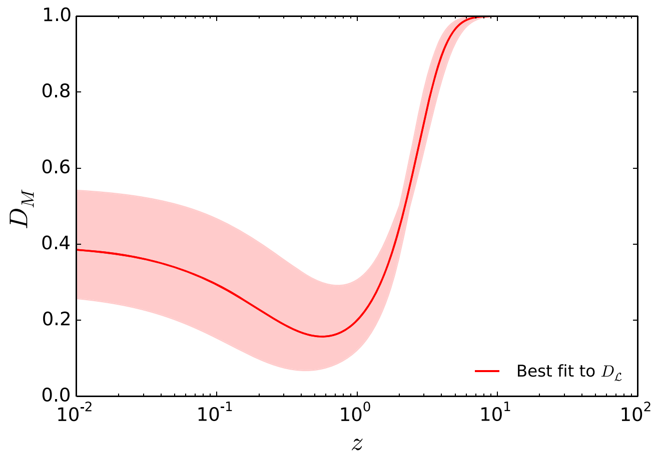

Figure 1. Depletion function $D_M(z)$ determined from the optimizing the fit to the low- and high-z $D_{\mathcal{L}}$ data in figure 2.

$$D_M(z) = 1 - (1 + e^{(z-z_0)/\tau})^{-1} + Ae^{-z/b}. \tag{2}$$

Here, z_0 is the redshift characterizing the large-scale structure formation epoch and τ its duration. A is the mass fraction of structures whose shapes have evolved into more symmetric ones (e.g. disk galaxies merging to form elliptical galaxies) and b is the duration of that evolution process. Figure 1 displays $D_M(z)$, for values $z_0 = 2.20 \pm 0.18$, $\tau = 0.84^{+0.15}_{-0.19}$, $A = 0.33 \pm 0.09$, and $b = 0.20^{+0.15}_{-0.05}$. A similar plot is found in Deur 2022, albeit using slightly different parameters determined from the CMB anisotropy spectrum.

3. The Hubble tension from the GR-SI perspective

A Hubble tension arising within ΛCDM is expected from the perspective of GR-SI: H_0 affects the observation of the CMB anisotropies essentially via the angular diameter distance of last scattering, d_A. This quantity depends upon the evolution of the Universe similarly to the luminosity distance $D_{\mathcal{L}}$ that enters the lower-z determination of H_0, e.g. via supernova observations. Specifically, $d_A(z) = D_{\mathcal{L}}(z)/(1+z)^2$. For example, in the ΛCDM model,

$$d_A(z) = \frac{1}{H_0(1+z)\sqrt{\Omega_K}} \sinh\left(\sqrt{\Omega_K} \int_{(1+z)^{-1}}^{1} \frac{dx}{\sqrt{\Omega_\Lambda x^4 + \Omega_K x^2 + \Omega_M x + \Omega_\gamma}}\right), \tag{3}$$

$$D_{\mathcal{L}}(z) = \frac{(1+z)}{H_0\sqrt{\Omega_K}} \sinh\left(\sqrt{\Omega_K} \int_{(1+z)^{-1}}^{1} \frac{dx}{\sqrt{\Omega_\Lambda x^4 + \Omega_K x^2 + \Omega_M x + \Omega_\gamma}}\right), \tag{4}$$

with Ω_Λ, Ω_M and Ω_γ the dark energy, total matter and radiation densities relative to the critical density, respectively, and $\Omega_K \equiv K/a_0^2 H_0^2$ with K the curvature and a_0 the Friedmann-Lemaître-Robertson-Walker scale factor at present time. Therefore, the determination of H_0 from CMB observations is analogous to a highly accurate $D_{\mathcal{L}}(z_L)$ observation, where z_L is the redshift at the time of last rescattering. Figure 2 depicts two luminosity distances $D_{\mathcal{L}}(z)$ calculated within ΛCDM with $\Omega_\Lambda = 0.69$, $\Omega_M = 0.31$ and $K = 0$, but different H_0 values: 73.06 km/s/Mpc, which matches the supernova and γ-ray data at low-z (dashed blue line in the left panel and blue dots in the right), and the other with 67.28 km/s/Mpc to match the CMB $D_{\mathcal{L}}(z_L)$ (dotted green line and green points). The uncertainty of the CMB datum is adjusted to equalize the χ^2/ndf values of the fits for the comparison of the data and the two ΛCDM cosmologies. The Hubble tension is evident in the two ΛCDM curves which match well either the low-z data or the high-z datum, but not both. However, the GR-SI model for $D_{\mathcal{L}}(z)$ (Deur 2019, 2022),

$$D_{\mathcal{L}}(z) = \frac{(1+z)}{\sqrt{\Omega_K} H_0} \sinh\left(\sqrt{\Omega_K} \int_{1/(1+z_L)}^{1} \frac{dx}{\sqrt{\Omega_K x^2 + D_M(1/x - 1)x}}\right), \tag{5}$$

fits both data sets well, as quantified by a significantly smaller χ^2/ndf value, thereby alleviating the discrepancy in estimating H_0 using different methods. Here, we elected to let the parameters of $D_M(z)$ be determined from the best fit to the $D_{\mathcal{L}}(z)$ data. This yields $z_0 = 2.20 \pm 0.18$, $\tau = 0.84^{+0.15}_{-0.19}$, $A = 0.33 \pm 0.09$ and $b = 0.24^{+0.10}_{-0.16}$ which is shown in figure 1. Originally the values of the parameters were obtained from the knowledge of the evolution of large-scale structures. The newfound values are smaller than the estimates from large structure formation $z_0 = 6.3^{+1.6}_{-2.0}$ and $\tau = 2.4^{+0.5}_{-0.3}$, but the ratio $z_0/\tau = 2.62$ happens to be the same for the fit and the estimates from

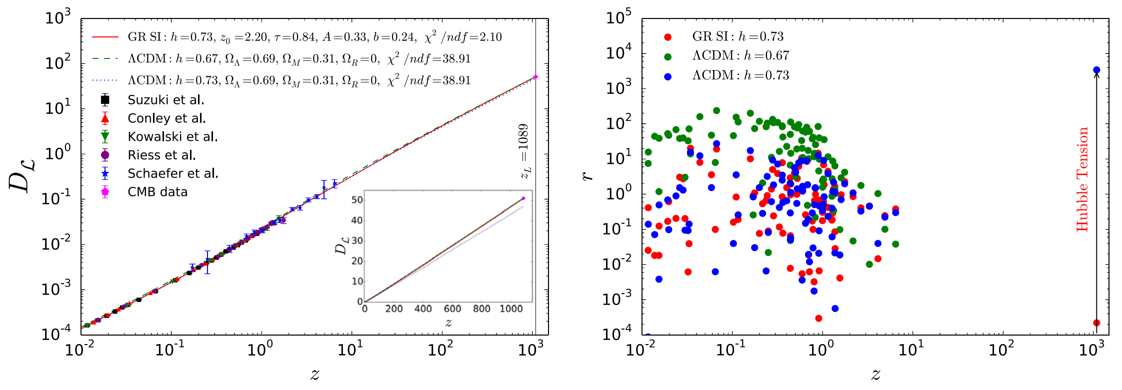

Figure 2. Left: Luminosity distance $D_\mathcal{L}$ as a function of redshift z for: ΛCDM using $h \equiv H_0/100$ km/s/Mpc $= 0.67$ (dashed green line) or h=0.73 (dotted blue line); and GR-SI with h=0.73 (solid red line). The embedded figure is the same but in linear rather than log scales. The low-z observational data (Riess *et al* 1998, Schaefer 2007, Kowalski *et al* 2008, Conley *et al* 2011, Suzuki *et al* 2012, Aghanim *et al* 2020b), shown by the square, triangle, circle and star symbols, are normalized using the $h = 0.73$ average low-z determination. The pentagon symbol shows $D_\mathcal{L}(z_L)$ as it would be obtained using the values of z_L and H_0 from the ΛCDM fit of the CMB. Right: Same as the left panel but for the normalized residual $r = (D_\mathcal{L} - d_{\rm obs})^2/e^2_{\rm obs}$, where $d_{\rm obs}$ is the observed data, $e_{\rm obs}$ their uncertainty, and the colors match that of the three different models used to compute $D_\mathcal{L}$ in the left panel. The Hubble tension appears as the offset between the ΛCDM curve which fits the low-z data (dotted blue line in the left panel and blue dots in the right panel) and the blue dot at z_L. The green dot at z_L is near $r = 0$ and hence not visible with the log scale.

large structure formation. The fit values for the A and b parameters agree with the earlier values, $A = 0.25^{+0.20}_{-0.17}$ and $b = 0.20^{+0.15}_{-0.05}$. In section 4, we verify that the CMB primary anisotropies remain well described with the H_0 and $D_M(z)$ determined by our best fit.

The $D_\mathcal{L}(z)$ calculated within ΛCDM and GR-SI differ chiefly at intermediate values of z because SI induces a large-distance suppression of gravity which curves $D_\mathcal{L}(z)$ in the $1 \lesssim z \lesssim 10$ domain, when large-scale structures start forming (Deur 2019, 2022).

The specific timing and amount of matter involved in the formation of large-scale structures result in the particular z-dependence of $D_M(z)$ which differs from the $\propto z^4$ effect of dark energy in ΛCDM. Thus, if SI noticeably influences the evolution of the Universe, there will arise a discrepancy with $D_\mathcal{L}(z)$ determinations using smaller-z phenomena for which the evolution spans a much smaller range. Since the determination of H_0 from the CMB is analogous to a determination using $D_\mathcal{L}(z_L)$, extracting H_0 from the CMB using the ΛCDM framework will cause a tension with H_0 measurements at lower z. The same applies to the baryonic acoustic oscillations (BAO) observation from the CMB. It is characterized by the acoustic horizon angular size, $\theta = d_H/d_A(z_L)$, where d_H is the acoustic horizon. Since d_H is the comoving distance travelled by a sound wave until recombination, *viz*, it happens for $z > z_L$ when the Universe was homogeneous and dark energy negligible, d_H is essentially the same for ΛCDM and GR-SI. It is the distinct evolution of $d_A(z)$ in ΛCDM and GR-SI that makes their θ predictions different. Like $D_\mathcal{L}$, d_A is predicted by ΛCDM to be larger at $z = 0$, yielding smaller θ and H_0 values compared to local measurements and the expectation from GR-SI.

4. Dependence of the CMB observation on the expansion of the Universe

While the $D_M(z)$ determined by the fit described in section 3 agrees qualitatively with that used for the CMB study in (Deur 2022), it differs quantitatively. Therefore, it is important for the internal consistency of the GR-SI model to verify that the CMB primary anisotropies remains well described with the present $D_M(z)$.

We will consider only the scalar multipole coefficient $C^s_{TT,l}$ since it is sufficient to investigate whether a Hubble tension is present in the GR-SI model. In particular, it is not necessary for the goal of this article to investigate the polarized CMB data. We use an analytical expression of the CMB anisotropies to show how the expansion of the Universe affects their observations at present-day. Such analytical expression is provided by the hydrodynamic approximation (Weinberg 2008). Despite not being as accurate as state-of-the-art numerical treatments of the CMB, this treatment is sufficient for the goal of this article, namely to investigate the Hubble tension within the GR-SI model. This is verified *a posteriori* by the small χ^2/ndf characterizing the GR-SI fits to the CMB. At z_L, the Universe is very homogeneous, making SI effects negligible. Thus, the phenomena that created the CMB anisotropies are unaffected and so are the mathematical expressions formalizing them. However, some of the parameters entering the CMB anisotropy expression use their present time values. They are thus affected by the expansion of the Universe and therefore contribute to the Hubble tension. In what follows, values of parameters at the present time, matter-radiation equilibrium time, and last scattering time are indicated by the subscripts 0, EQ and L, respectively. Baryon relative density is denoted by Ω_B, and, for ΛCDM,

Table 1. CMB quantities depending explicitly on the expansion of the Universe. Column 1: quantity. Column 2: ΛCDM expression. Column 3: GR-SI expression.

	ΛCDM	GR-SI
d_A	$\frac{1}{\sqrt{\Omega_K}H_0(1+z_L)}\sinh\left(\sqrt{\Omega_K}\int_{1/(1+z_L)}^{1}\frac{dx}{\sqrt{\Omega_\Lambda x^4+\Omega_K x^2+\Omega_M x}}\right)$	$\frac{1}{\sqrt{\Omega_K}H_0(1+z_L)}\sinh\left(\sqrt{\Omega_K}\int_{1/(1+z_L)}^{1}\frac{dx}{\sqrt{\Omega_K x^2+D_M(1/x-1)x}}\right)$
t_L	$\frac{1}{H_0}\int_0^{1/(1+z_L)}\frac{xdx}{\sqrt{\Omega_\Lambda x^4+\Omega_K x^2+\Omega_M x+\Omega_R}}$	$\frac{1}{H_0}\int_0^{1/(1+z_L)}\frac{xdx}{\sqrt{\Omega_K x^2+D_M(1/x-1)+\Omega_R]}}$

Table 2. Expressions of the quantities that are not explicitly dependent on the expansion of the Universe. Column 1: Quantity. Column 2: ΛCDM expression. Column 3: GR-SI expression. In these expressions, σ is the standard deviation for the temperature T_L, $Y \simeq 0.24$ is the density ratio of nucleons to neutral ^{4}He, σ_T is the Thompson cross-section, ρ_B and ρ_γ are average absolute densities of baryon and radiation, respectively, and n_{B0} is the baryon number density at present time.

	FLRW universe	Universe with GR's SI accounted for
d_T	$\sqrt{\Omega_R}/[(1+z_L)H_0\Omega_M]$	$\sqrt{\Omega_R}/[(1+z_L)H_0D_M(0)]$
R_L	$[3\Omega_B]/[4\Omega_\gamma(1+z_L)]$	Same as for ΛCDM
R_{EQ}	$[3\Omega_R\Omega_B]/[4\Omega_M\Omega_\gamma]$	$[3\Omega_R\Omega_B]/[4\Omega_M D(0)\Omega_\gamma]$
d_H	$\frac{2}{H_0(3R_L\Omega_M)^{1/2}(1+z_L)^{3/2}}\ln([\sqrt{1+R_L}+\sqrt{R_{EQ}+R_L}]\Big/[1+\sqrt{R_{EQ}}])$	$\frac{2}{H_0(3R_LD_M(0))^{1/2}(1+z_L)^{3/2}}\ln([\sqrt{1+R_L}+\sqrt{R_{EQ}+R_L}]\Big/[1+\sqrt{R_{EQ}}])$
d_D	$\sqrt{d^2_{\mathrm{Landau}}+d^2_{\mathrm{Silk}}}$	Same as for ΛCDM
d^2_{Landau}	$\frac{3\sigma^2t_L^2}{8T_L^2(1+R_L)}$,	Same as for ΛCDM
d^2_{Silk}	$\frac{R_L^2}{6(1-Y)(n_{B0})\sigma_T H_0\sqrt{\Omega_M}R_0^{9/2}}\int_0^{R_L}\frac{R^2dR}{X(R)(1+R)\sqrt{R_{EQ}+R}}\left[\frac{16}{15}+\frac{R^2}{1+R}\right]$	$\frac{R_L^2}{6(1-Y)(n_{B0})\sigma_T H_0\sqrt{D_M(0)}R_0^{9/2}}\int_0^{R_L}\frac{R^2dR}{X(R)(1+R)\sqrt{R_{EQ}+R}}\left[\frac{16}{15}+\frac{R^2}{1+R}\right]$
$R(t)$	$^{3\rho_B(t)}\big/4\rho_\gamma(t)$	Same as for ΛCDM
$X(T)$	$1\Big/\left[X^{-1}(3400)+\frac{\Omega_Bh^2}{(\Omega_Mh^2)^{1/2}}\int_T^{3400}g(T')dT'\right]$	$1\Big/\left[X^{-1}(3400)+\frac{\Omega_Bh^2}{(D_M(0)h^2)^{1/2}}\int_T^{3400}g(T')dT'\right]$

the dark matter relative density is Ω_{DM}. We consider $C^s_{TT,l}$, the scalar multipole coefficient for the temperature-temperature angular correlation (here l is the multipole moment). Its expression within the *hydrodynamic approximation* is provided in (Weinberg 2008):

$$\frac{l(l+1)C^s_{TT,l}}{2\pi}=\frac{4\pi T_0^2N^2e^{-2\tau_{reion}}}{25}\int_1^\infty d\beta\left(\frac{\beta l}{l_{\mathcal{R}}}\right)^{n_s-1}$$
$$\times\left\{\frac{3\sqrt{\beta^2-1}}{\beta^4(1+R_L)^{3/2}}\mathcal{S}^2(\beta l/l_T)e^{-2\beta^2l^2/l_D^2}\sin^2(\beta l/l_H+\Delta(\beta l/l_T))\right.$$
$$\left.+\frac{1}{\beta^2\sqrt{\beta^2-1}}[3\mathcal{T}(\beta l/l_T)R_L-(1+R_L)^{-1/4}\mathcal{S}(\beta l/l_T)e^{-\beta^2l^2/l_D^2}\cos(\beta l/l_H+\Delta(\beta l/l_T))]^2\right\}+\mathcal{C}(l). \tag{6}$$

The first term in the curly bracket formalizes the Doppler effect. The second term provides the Sachs-Wolf and intrinsic temperature anisotropy effects. Both terms also contains the large-l damping. N is the normalization of the primordial perturbations, τ_{reion} is the reionized plasma optical depth, β is an integration variable akin to a wave number, n_s is the scalar spectral index, $l_{\mathcal{R}} \equiv (1+z_L)k_{\mathcal{R}}d_A$ is a multipole characteristic value, with $k_{\mathcal{R}} \equiv 0.05\ \mathrm{Mpc}^{-1}$ a conventional scale. Other multipole characteristic values are $l_T = d_A/d_T$ (d_T is a length scale whose form differs in ΛCDM and GR-SI; see below), $l_D = d_A/d_D$ (d_D is the damping length) and $l_H = d_A/d_H$. $R_L = 3\Omega_B/4\Omega_\gamma(1+z_L)$ is a ratio of relative densities and $\mathcal{S}$, $\mathcal{T}$ and Δ are transfer functions. Finally, $\mathcal{C}(l)$ is a second-order term correcting the approximations of the hydrodynamic model (Deur 2022). Hereafter, since $\mathcal{C}(l)$ is small, we will ignore its possible dependence on the difference between the Universe evolutions according to ΛCDM and GR-SI.

The integrated Sachs-Wolf, Sunyaev-Zel'dovich and cosmic variance effects, which produce anisotropies that are extrinsic to the CMB origin, are not included in the hydrodynamic model. This does not affect our study of the Hubble tension since we will focus on the multipole range $48 < l < 1800$, a domain where these effects are unimportant.

In equation (6), the quantities that depend on the expansion of the Universe are integrated over z. There are only two such parameters: d_A and t_L. Their expressions in ΛCDM and GR-SI are given in table 1. The expressions of the quantities not explicitly affected by the expansion of the Universe are tabulated in table 2 for convenience. Some of these quantities depend indirectly on the expansion of the Universe as they contain t_L, z_L or d_A, namely d_T, R_L, d_{Landau}, d_{Silk}, d_H and d_D (the latter through d_{Landau} and d_{Silk}), $l_{\mathcal{R}}$, l_T, l_D and l_H. In all, this shows that the Hubble tension may be cast as the problem of properly modeling the distances d_A and $D_{\mathcal{L}}$. In fact, once SI is

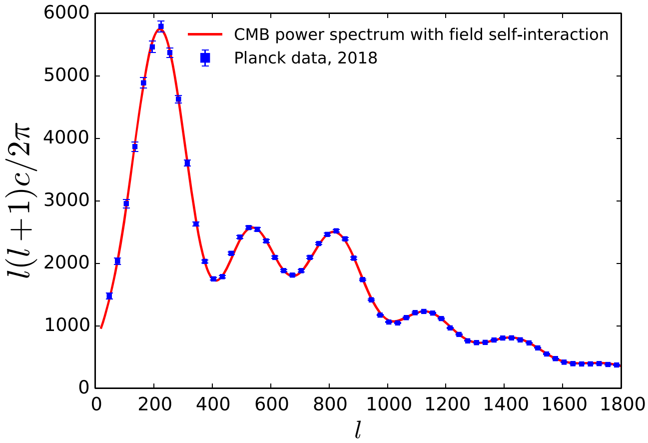

Figure 3. Power spectrum of the CMB temperature anisotropy. The continuous line is $l(l+1)C^s_{TT,l}/(2\pi)$ computed using GR-SI with the low-z average for the Hubble parameter, H_0=73.06 km/s/Mpc. The squares are the Planck measurement (Aghanim *et al* 2020b, 2018 release).

accounted for in the CMB anisotropy expression, we can fit the $C^s_{TT,l}$ data while keeping H_0 to its low-z determination of 73.06 km/s/Mpc and the $D_M(z)$ parameters obtained from the best fit of $D_{\mathcal{L}}(z)$ (red line of figure 1). The parameters allowed to vary are z_L, N, n_s, σ and Ω_B, with the $C^s_{TT,l}$ spectrum reproduced for $z_L = 1728 \pm 1$, $N = (1.1995 \pm 0.0019) \times 10^{-5}$, $n_s = 0.9759 \pm 0.0028$, $\sigma = 1.751 \pm 0.0002$ and $\Omega_B h^2 = 0.0370 \pm 0.0002$, with $\chi^2/ndf = 0.5$, see figure 3. We remark that the quoted uncertainties are only fit uncertainties and do not include other systematic effects, e.g. coming from approximations in the CMB hydrodynamics model or from the choice of functional form for $D_M(z)$ and its parameters. This fit must use the H_0 value determined by low-z observations since it is the value of H_0 in the GR-SI model, consistent with the value obtained from $D_{\mathcal{L}}(z_L)$ once the Universe expands accordingly to that model. This is verified by performing a CMB fit with H_0=67.28 km/s/Mpc and observing that the χ^2/ndf of that fit is larger (by about 20%) than that of the nominal fit. It is also interesting to perform the fit with H_0 kept a free parameter despite the fact that it introduces a slight inconsistency since the determination of the $D_M(z)$ parameters is obtained with the H_0 value fixed by $z \simeq 0$ observations. Such fit yields $H_0 = 72.99 \pm 0.06$ km/s/Mpc, $z_L = 1728 \pm 1$, $N = (1.2014 \pm 0.0015) \times 10^{-5}$, $n_s = 0.9738 \pm 0.0027$, $\sigma = 1.751 \pm 0.002$ and $\Omega_B h^2 = 0.0368 \pm 0.0002$, with $\chi^2/ndf = 0.58$.

5. Conclusion

Our results show consistency between SnIA and CMB-determined H_0 values if one accounts, when quantifying the evolution of the Universe, for the self-interaction of gravitational fields, a feature of General Relativity ordinarily neglected. It is the first step toward resolving the Hubble tension. A full resolution of the tension requires additional steps: confirming that for a given set of cosmological parameters there is *simultaneous* agreement between GR-SI theory and observations, such as those of the matter power spectrum or the rate of growth of structure σ_8. In the cosmological model used in this article, as in the previous studies using that model, the effects of self-interaction are contained within a depletion function which effectively relaxes the traditional assumptions of the Cosmological Principle—isotropy and homogeneity of the evolving universe. Here, the parameters of the depletion function are determined from the best fit to the luminosity distance data, a procedure that appears more accurate than the method used in (Deur 2019), *viz*, determining the parameters from our knowledge of the timescale at which large-scale structures form, and of the amount of baryonic matter present in these structures. We show that the resulting luminosity distance fits simultaneously both low-redshift supernovae data as well as high-redshift CMB data. Furthermore, the GR-SI model, with the depletion function thus determined, fits well the CMB power spectrum data. This shows that determining the depletion function using low-z and high-z values of the luminosity distance did not create an internal inconsistency within the GR-SI model, as far as the CMB spectrum is concerned. Therefore, simultaneous close fits with the same value of H_0 of both low-z and high-z luminosity data on the one hand and CMB spectrum data on the other exhibits no Hubble tension within the GR-SI model. Crucially, The large-distance suppression of gravity, *viz*, the *global* effect, is evaluated effectively using a *depletion function* $D_M(z)$ that originates from lifting the traditional assumptions that the Universe is isotropic and homogeneous (Deur 2019). If $D_M = 0$, gravity is fully quenched at large-distance while for D_M=1 there is no net SI effect. Thus, $D_M(z) \approx 1$ for the early universe since it was nearly isotropic and homogeneous. In contrast, the large-scale structures of the present universe entail $D_M(z \approx 0) < 1$. this harmonization of the SnIA and CMB H_0 determinations does not require adding parameters beyond those already present in the model. This is important because in order to be a compelling alternate to ΛCDM, a model should display a consistency and simplicity on par with ΛCDM, i.e. it should avoid introducing too many new and ad-hoc parameters, particles or fields. This is the case for the model used here which requires no new physics beyond the standard model of particle physics and General Relativity. Reconciling the late- and early-universe H_0 values did not compromise this attractive feature of the model.

Acknowledgments

This publication is dedicated to the memory of Corey Sargent, who tragically passed away on June 11, 2022, at the age of 25, and to his parents, Tracy Sargent and Gerard Carelli. At the time of his passing, Corey had just started his work on the project that lead to this article. For his Ph.D supervisors, A D and B T, he was the engine of their nascent astrophysics group at Old Dominion University, and one of the brightest students they ever worked with despite their long experience with talented students. For his fellow student W C he was a friend and a mentor.

This work is done in part with the support of the U S National Science Foundation award No. 1847771. The authors are grateful to A Mand and T Möller for their useful comments on the manuscript.

Data availability statement

All data that support the findings of this study are included within the article (and any supplementary files).

ORCID iDs

Alexandre Deur https://orcid.org/0000-0002-2203-7723
Balša Terzić https://orcid.org/0000-0002-9646-8155

References

Abdalla E *et al* 2022 *JHEAp* **34** 49
Aghanim N *et al* 2020a *Astron. Astrophys.* **641** A6
Aghanim N *et al* 2020b *Astron. Astrophys.* **641** A5
Alam S *et al* 2021 *Phys. Rev.* D **103** 083533
Arcadi G *et al* 2018 *Eur. Phys. J.* C **78** 203
Banik I *et al* 2023 *Mon. Not. R. Astron. Soc.* **527** 4573–4615
Banik I and Zhao H 2018 *Mon. Not. R. Astron. Soc.* **480** 2660
Chae K-H 2023 *Astrophys. J.* **956** 69
Conley A *et al* 2011 *Astrophys. J. Suppl.* **192** 1
Deur A 2009 *Phys. Lett.* B **676** 21
Deur A 2014 *Mon. Not. R. Astron. Soc.* **438** 1535
Deur A 2017 *Eur. Phys. J.* C **77** 412
Deur A 2019 *Eur. Phys. J.* C **79** 883
Deur A 2021a *Eur. Phys. J.* C **81** 213
Deur A 2021b *Phys. Lett.* B **820** 136510
Deur A 2022 *Class. Quant. Grav.* **39** 135003
Deur A, Brodsky S J and de Teramond G F 2016 *Prog. Part. Nucl. Phys.* **90** 1
Deur A, Sargent C and Terzić B 2020 *Astrophys. J.* **896** 94
Di Valentino E *et al* 2021 *Class. Quant. Grav.* **38** 153001
Fierz M and Pauli W 1939 *Proc. Roy. Soc. Lond.*A **173** 211
Freedman W L *et al* 2020 *Astrophys. J.* **891** 57
Gaskins J M 2016 *Contemp. Phys.* **57** 496
Gross F *et al* 2023 *Eur. Phys. J.* C **83** 1125
Kahlhoefer F 2017 *Int. J. Mod. Phys.* A **32** 1730006
Klypin A A, Kravtsov A V, Valenzuela O and Prada F 1999 *Astrophys. J.* **522** 82
Kowalski M *et al* 2008 *Astrophys. J.* **686** 749
Macpherson H J, Lasky P D and Price D J 2018 *Astrophys. J. Lett.* **865** L4
Macpherson H J, Price D J and Lasky P D 2019 *Phys. Rev.* D **99** 063522
McGaugh S S, Lelli F and Schombert J M 2016 *Phys. Rev. Lett.* **117** 201101
Riess A G *et al* 1998 *Astron. J.* **116** 1009
Riess A G *et al* 2016 *Astrophys. J.* **826** 56
Riess A G, Yuan W, Macri L M *et al* 2022 *Astrophys. J. Lett.* **934** L7
Sancisi R 2004 The Visible matter - Dark matter coupling *IAU Symp.* 220, 233
Schaefer B E 2007 *Astrophys. J.* **660** 16

Schander S and Thiemann T 2021 *Front. Astron. Space Sci.* **8** 113
Shah P, Lemos P and Lahav O 2021 *The Astronomy and Astrophysics Review* **29** 1
Suzuki N *et al* 2012 *Astrophys. J.* **746** 85
Tully R B and Fisher J R 1977 *Astronomy and Astrophysics* **54** 661
Verde L, Treu T and Riess A G 2019 *Nature Astron.* **3** 891
Weinberg S 2008 *Cosmology* (Oxford University Press)
Wilczek F 2002 Four big questions with pretty good answers *Werner Heisenberg Centennial Symposium Developments in Modern PhysicsFundamental physics - Heisenberg and beyond.* ed Buschhorn and Wess pp 79–97
Winters D, Deur A and Zheng X 2023 *Mon. Not. Roy. Astron. Soc.* **518** 2845
Wong K C *et al* 2020 *Mon. Not. Roy. Astron. Soc.* **498** 1420
Zee A 2013 *Einstein Gravity in a Nutshell* (Princeton University Press)